

This article was downloaded by: [Tomsk State University of Control Systems and Radio]

On: 21 February 2013, At: 12:02

Publisher: Taylor & Francis

Informa Ltd Registered in England and Wales Registered Number: 1072954

Registered office: Mortimer House, 37-41 Mortimer Street, London W1T 3JH, UK



Molecular Crystals and Liquid Crystals

Publication details, including instructions for authors and subscription information:

<http://www.tandfonline.com/loi/gmcl16>

Dependence of polymer electronic structure on molecular architecture

C. B. Duke^a, A. Paton^a & W. R. Salaneck^a

^a Xerox Webster Research Center Xerox Square-114, Rochester, N.Y., 14644

Version of record first published: 14 Oct 2011.

To cite this article: C. B. Duke, A. Paton & W. R. Salaneck (1982): Dependence of polymer electronic structure on molecular architecture, *Molecular Crystals and Liquid Crystals*, 83:1, 177-197

To link to this article: <http://dx.doi.org/10.1080/00268948208072168>

PLEASE SCROLL DOWN FOR ARTICLE

Full terms and conditions of use: <http://www.tandfonline.com/page/terms-and-conditions>

This article may be used for research, teaching, and private study purposes. Any substantial or systematic reproduction, redistribution, reselling, loan, sub-licensing, systematic supply, or distribution in any form to anyone is expressly forbidden.

The publisher does not give any warranty express or implied or make any representation that the contents will be complete or accurate or up to date. The accuracy of any instructions, formulae, and drug doses should be independently verified with primary sources. The publisher shall not be liable for any loss, actions, claims, proceedings, demand, or costs or damages

whatsoever or howsoever caused arising directly or indirectly in connection with or arising out of the use of this material.

Mol. Cryst. Liq. Cryst., 1982, Vol. 83, pp. 177-197
0026-8941/82/8301-0177\$06.50/0
© 1982 Gordon and Breach, Science Publishers, Inc.
Printed in the United States of America

(Proceedings of the International Conference on Low-Dimensional Conductors, Boulder, Colorado, August 1981)

DEPENDENCE OF POLYMER ELECTRONIC STRUCTURE ON MOLECULAR ARCHITECTURE

C.B. DUKE, A. PATON AND W.R. SALANECK
Xerox Webster Research Center
Xerox Square-114, Rochester, N.Y., 14644

Submitted for publication August 21, 1981

A review of the influence of macromolecular architecture on the electronic structure of polymers is presented. Calculations of the density of valence electron states (DOVS) based on the CNDO/S3 molecular orbital model are presented for polyacetylene, poly(p-phenylene), poly(p-phenylene vinylene), poly(p-phenylene sulfide), poly(2,5-thienylene), poly(1,6 heptadiyne), and poly(p-xylylene). These DOVS are shown to provide good descriptions of measured valence electron photoemission spectra in all cases for which such spectra are available. The model is applied to demonstrate the occurrence of short chain segments in mixed cis-trans polyacetylene. Relationships between macromolecular architecture and characteristic features in the photoemission spectra are demonstrated. In particular, criteria leading to extended pi-electron states are identified.

INTRODUCTION

In recent years considerable effort has been devoted to modifying the electrical properties of polymers by doping. Several distinct applications of such materials have been envisaged, including photoconductors, conductors, and battery electrodes. Perhaps the most important new-materials design issue is the selection of the host polymer so that the resultant doped material exhibits chemical stability, mechanical flexibility, and ease of processing as well as the desired electrical

properties. To achieve this combination of properties, a number of host polymers have been examined including polyacetylene $[(CH)_x]$, poly(p-phenylene) $[(C_6H_4)_x]$, poly(2,5-thienylene) $[C_4SH_2]_x$, poly(1,6-heptadiyne) $[(CH(C_6H_7))_x]$, poly(p-phenylene sulfide) $[(C_6H_4S)_x]$, poly(p-phenylene oxide) $[(C_6H_4O)_x]$, poly(p-xylylene) $[(C_6H_4C_2H_4)_x]$, and poly(p-phenylene vinylene) $[(C_6H_4C_2H_2)_x]$, as described in several recent reviews.

Our purpose in this article is to examine the dependence of the electronic structure of such host polymers on their molecular architecture. We focus our attention on the density of valence-electron states (DOVS) because this quantity is measurable by photoemission spectroscopy.⁵ It is known that even in the best of cases the DOVS and photoemission spectra do not change for oligomers longer than approximately ten repeat units.^{4,6-8} Therefore we confine our attention to oligomers of sufficient size that the associated DOVS do not change upon increasing their length further. Our calculations are based upon the spectroscopically parameterized CNDO/S3 molecular orbital model whose construction and verification for "small" molecules is documented elsewhere.⁹ The dependence of polymer electronic properties on polymer structure also has been examined by other authors,^{10,11} and a preliminary account of our work already has appeared.⁶ Our approach differs from those of others^{10,11} by virtue of our focus on calculations of quantities which are directly measurable by photoelectron spectroscopy.

On the basis of our work we propose four major conclusions. First, the pi-electron states in polyacetylene are almost invariant under changes in molecular conformation between the various cis and trans forms. This bodes well for conductivity in these systems because it suggests that conformational disorder is not effective in breaking up the pi-electron wavefunctions. Second, we find that the nature of the occupied valence electron states for unsaturated ring systems (e.g., phenyl moieties) connected by saturated bonds [e.g., poly(p-phenylene), poly(2,5-thienylene), poly(p-xylylene)] are essentially different in character from those of acetylene-based systems [e.g., polyacetylene, poly(1,6-heptadiyne)]. Their pi electron states are divided into a narrow "non-bonding" pi-band (which is quite prominent in photoemission spectra) and a wider "bonding" pi band. The width of this latter band is quite sensitive to the length and conformation of the linkage between rings, ranging from quite large (~ 3 eV) for planar poly(p-phenylene) to less than a few tenths of an eV for poly(p-xylylene). Thus, this band is sensitive to conformational disorder. Moreover, the presence of heteroatoms [(e.g.,

in poly(2,5-thienylene)] can fragment this band, and thereby render it more analogous to that in polyacetylene than to that in poly(p-phenylene). Third, the nature of the valence electron states for unsaturated ring systems connected by unsaturated or lone-pair linkages [e.g., poly(p-phenylene vinylene), poly(p-phenylene oxide), poly(p-phenylene sulfide)] are distinct from both of the other two classes of polymer. In these materials the bonding pi-electron orbitals of the ring system hybridize with the pi or lone-pair orbitals of the linkages and create bands whose width and character depends explicitly on the nature and extent of the hybridization. Fourth and finally, we find that the pi-electron states of polymers whose ring systems are coupled by two or more saturated $-\text{CH}_2-$ links are localized on the individual rings by the disorder inherent in typical polymeric solids. Examples of these systems are polystyrene, poly(p-xylylene) and poly(2-vinyl pyridine). Such systems would not be expected to be good candidates for conducting polymers if extended pi-electron states along the backbone are required for high conductivity. They are, however, quite suitable for electrophotographic applications for which hopping conductivity yields adequate device performance.

We proceed by defining our model calculations in the next section and then considering polyacetylene-like systems, aromatic ring systems with saturated linkages, and aromatic ring systems with non-saturated linkages, in turn. We conclude with a synopsis of our results.

MODEL CALCULATIONS

All of our calculations were performed for electrically neutral molecules using the CNDO/S3 molecular orbital model. The molecular orbital eigenvalues of the neutral species are identified with the associated molecular cation energies in accordance with the procedures developed during the construction of this model. Since a review of the details and applications of the model recently has been given by Duke,⁹ we do not recapitulate them here. The parameters used in the calculations [as described in Ref. 9] are given in Table I.

Comparison between the CNDO/S3 model calculations and measured photoemission spectra is achieved via plots of the density of valence states, i.e., "DOVS." These plots are obtained by representing each CNDO/S3 eigenvalue by a normalized gaussian of width β and weight equal to twice the degeneracy of the eigenvalue. For typical gas-phase photoemission spectra $0.2 \text{ eV} \leq \beta \leq 0.3 \text{ eV}$, whereas for photo-

TABLE I. Parameters used to define the CNDO/S3 model. The interatomic Coulomb integrals are specified in terms of their intra-atomic values (γ_A, γ_B) and the distance between the atomic centers (R_{AB}) via $\gamma_{AB} = 14.397 [28.794(\gamma_A + \gamma_B)^{-1} + R_{AB}]^{-1}$.

Atom	I_s (eV)	I_p (eV)	β_s (eV)	β_p (eV)	γ (eV)	ζ (A ⁻¹)
H	13.60	-----	10	--	12.85	2.33
C(sp ²)	21.34	11.54	20	17	10.63	3.78
C(sp ³)	21.34	11.54	20	17	10.63	3.07
O	35.50	17.91	31	26	13.10	4.32
S	21.02	10.97	18	15	9.67	4.37(s) 3.80(p)

emission from polymers and molecular solids 0.4 eV $\leq \beta \leq 1$ eV.^{4,7,12} The large values of β for condensed molecular phases have the consequence that for polymers such as polyacetylene photoemission from oligomers becomes identical to that from macromolecules when the oligomers contain 16-20 carbon atoms in the backbone chain. Therefore it is not possible to verify via photoemission spectroscopy phase coherence within macromolecules over distances greater than about 25Å. In the other polymers considered here even smaller oligomers give photoemission spectra essentially identical to those of the polymer. A complete theory of the widths of photoemission lines from polymers and molecular solids has been constructed elsewhere^{12,13} and shown to describe both the magnitude¹³ and temperature dependence¹⁴ of observed spectra. This theory reveals that the large values of $\beta \sim 0.6$ eV for polymers are associated in part with the photoemission process itself¹² and in part with the disordered nature of the polymeric solid state.^{12,13} Hence, from the perspective of photoemission spectroscopy, oligomers containing 16 or more backbone carbon species are indistinguishable from macromolecules.

POLYACETYLENE-LIKE SYSTEMS

Polyacetylene-like systems are polymers whose non-saturated backbone configuration is that of polyacetylene, i.e., alternating double and single bonds, a planar conformation, and 120° bond angles. In our calculations we use 1.35Å for the length of the double bond and 1.44Å for that of the single bond.¹⁵ The materials in this class for which we have performed calcula-

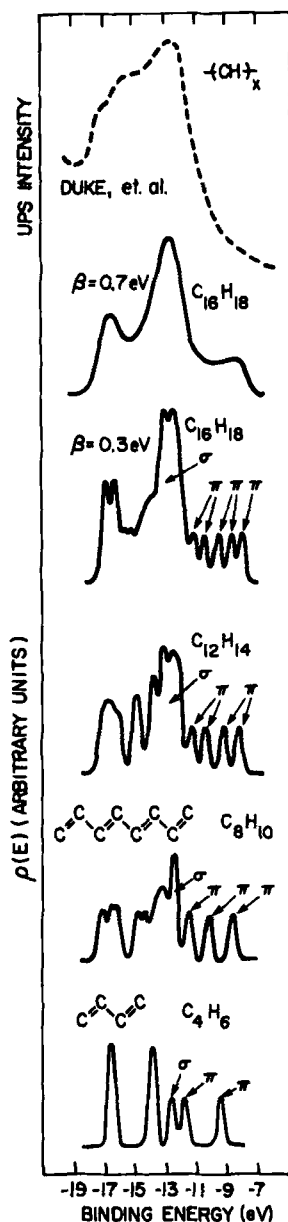
tions are polyacetylene itself and poly(1,6-heptadiyne).

One of our major interests in polyacetylene is the influence on the DOVS of the conformation of the $(\text{CH})_x$ chain. We have shown elsewhere⁶ that the pi-electron molecular ion energies are almost unaffected by conformational changes between the various cis and trans forms. The sigma molecular ion energies, on the other hand, are quite sensitive to the conformation of the polymer, and are suitable for use as fingerprints of the molecular conformation.¹⁶

Another important aspect of photoemission from polyacetylene is the assessment of the spatial extent of molecular cation states generated by a photoionization event. For this purpose we show in Fig. 1 the evolution of the DOVS of trans- $\text{H}(\text{CH})_n\text{H}$ as a function of n . The emergence of the $\pi(\pi)$ -electron band in the energy region $-11 \text{ eV} \leq E \leq -7 \text{ eV}$ and of a sigma-electron band in the region $-17 \text{ eV} \leq E \leq -11 \text{ eV}$ is evident from the figure. For typical solid-state width parameters, i.e., $\beta = 0.7 \text{ eV}$, the calculated DOVS remain invariant under increasing n for $n \geq 16$. Thus, we infer from the comparison of the calculated DOVS and the observed ultraviolet photoemission spectrum (UPS) shown in Fig. 1 that in the sigma bands and the center of the pi band the molecular ion states extend over at least 16-20 carbon atoms in the $(\text{CH})_x$ backbone. The absence of the predicted small shoulder at the low-binding-energy threshold of the photoemission spectrum implies that the photoinduced cation states at the upper edge of the $(\text{CH})_x$ pi electron valence band are localized by disorder.^{4,6} From the lower three panels of Fig. 1, we estimate that the "band-edge" states are localized to within $n \leq 10$ carbon atoms, in contrast to the values $n \geq 16$ characteristic of the center of the pi and sigma electron bands. Finally, comparing the photoemission spectrum in Fig. 1 with the calculations for $\text{H}(\text{CH})_{16}\text{H}$ indicates that the $(\text{CH})_x$ chains in the sample occur predominantly the trans configuration over spatial distances of at least 20 carbon atoms: a result inferred independently from the optical properties of the sample.

An interesting application of these ideas about localization is the study of the cis to trans isomerization which occurs when films of polyacetylene¹⁷ are heated following their synthesis at low temperatures. The ultraviolet photoemission spectra change with variations in the cis-trans content, as shown in Fig. 2.¹⁹ An indication of the photoelectron spectra of the cis polyacetylene remaining when the isomerization is 60% complete may be obtained by subtracting an appropriately weighted (i.e., by 0.6 in this case) spectrum of the all-trans material¹⁹ from that of the mixed cis-trans isomer. The results¹⁹ of this procedure are shown in Fig. 3 in which the

FIGURE 1. Calculated CNDO/S3 DOVS for a series of trans even polyenes. In the lower four panels a value of $\beta = 0.3$ eV was used to obtain the DOVS from the CNDO/S3 eigenvalue spectrum, corresponding to the analysis of photoemission from individual molecules in the gas phase. The top panel contains the measured ultraviolet photoemission spectrum of a film of $(CH)_x$ shifted to higher binding energies by 2.5 eV in order to preserve the same energy scale in all of the figures. Finally, the panel below contains the CNDO/S3 DOVS for trans- $H(CH)_{16}H$ evaluated using $\beta = 0.7$ eV corresponding to the solid state. If $\beta = 0.7$ eV, the DOVS for $H(CH)_mH$ do not differ noticeably from that for $H(CH)_{16}H$ for $m \geq 16$.



resulting difference spectra also are compared with model calculations of the DOVS.^{6,18} It is evident from this figure that the C_8H_{10} DOVS provides a good qualitative description of the difference spectrum, suggesting that the remaining segments of polyacetylene are about eight carbon atoms long. Merging this finding with other data to provide a self consistent model of the lengths and connectivities of the polymer chains in fibrillar polyacetylene is a complex task, however, because not all of the available spectroscopic data are internally consistent. Nevertheless, the analysis reveals clearly the level of structural detail which can be extracted

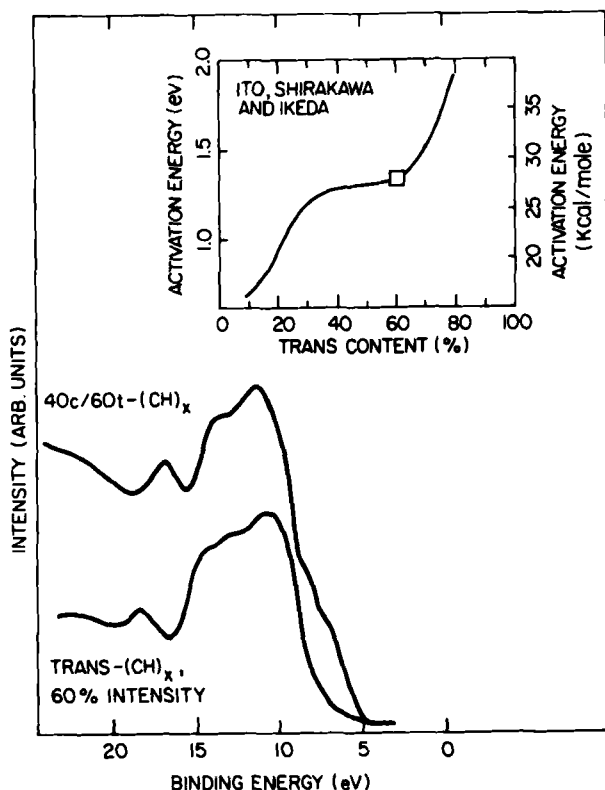


FIGURE 2. UPS spectra, obtained with synchrotron radiation at 40.0 eV photon energy, of $40c/60t-(CH)_x$ and $trans-(CH)_x$ are shown normalized for the appropriate subtraction. The inset shows an activation energy versus trans composition curve for $(CH)_x$ from Ito, Shirakawa and Ikeda.¹⁴

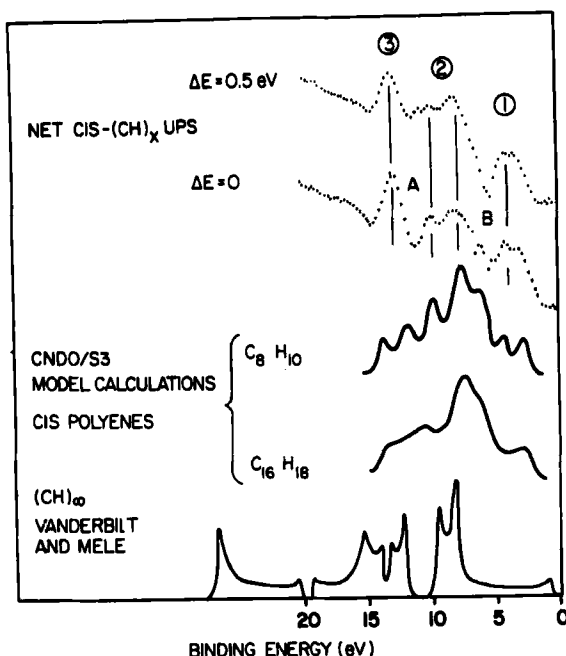
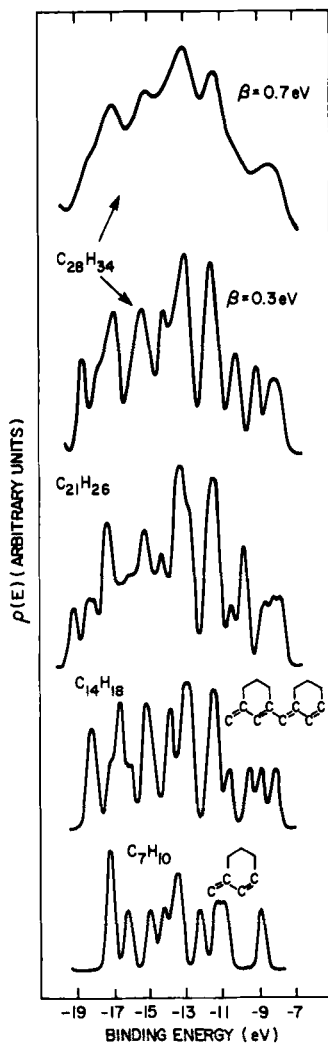


FIGURE 3. Difference curve for the cis-(CH)_x portion of the 40c/60t-(CH)_x spectrum. One extreme of a^x shift of the relative energies of the spectra of Fig. 1 before subtraction, $\Delta E = 0.5$ eV, is seen to make inconsequential modifications in the major features of the difference spectra. The density of states curve for "infinitely" long-chain trans-cisoid-(CH)_x is from Vanderbilt and Mele.¹⁸ The DOVS for finite cis polyenes calculated using the CNDO/S3 model⁹ are shown to illustrate that the major features of the difference spectra are predicted by this model for C₈H₁₀.

from analyses of valence-electron photoemission spectra using spectroscopically validated molecular orbital models.

Turning to poly(1,6-heptadiyne), the focus of our interest is the influence on the DOVS of the changes in electronic structure wrought by the propyl side groups. We show in Fig. 4 the evolution of the DOVS for poly(1,6-heptadiyne) as a function of *n* in the series of model molecules trans - H[CH(C₆H₇)]_n H. Thus, Fig. 4 for poly(1,6-heptadiyne) is the precise analog of Fig. 1 for polyacetylene. It is evident that the substituents induce substantial changes in both the pi- and sigma-electron contributions to the DOVS, leading to profound

FIGURE 4. Calculated CNDO/S3 DOVS for a series of substituted even-polyenes, $H[CH(C_6H_7)]_nH$ ($n=1,2,3$ and 4) which become poly(1,6-heptadiyne) in the limit of large n . The value $\beta = 0.3$ eV for the width parameter was used to obtain the spectra shown in the lower four panels whereas the solid-state value, $\beta = 0.7$ eV, was utilized to construct the uppermost-panel for $H[CH(C_6H_7)]_4H$.



alternations in the DOVS relative to that of polyacetylene. Consequently, although the $(-CH=CH-)$ chain in the backbone of trans- poly(1,6-heptadiyne) is nearly identical in structure to that of polyacetylene, its electronic structure is discernably different. We also predict a small red shift by about the main $\pi \rightarrow \pi$ absorption band of poly(1,6-heptadiyne) relative to that of polyacetylene. Moreover, poly (1,6-heptadiyne) is predicted to be more susceptible to chemical attack because the backbone carbon species attached to side-group carbons exhibit an electron deficiency of only 0.06e relative to a value

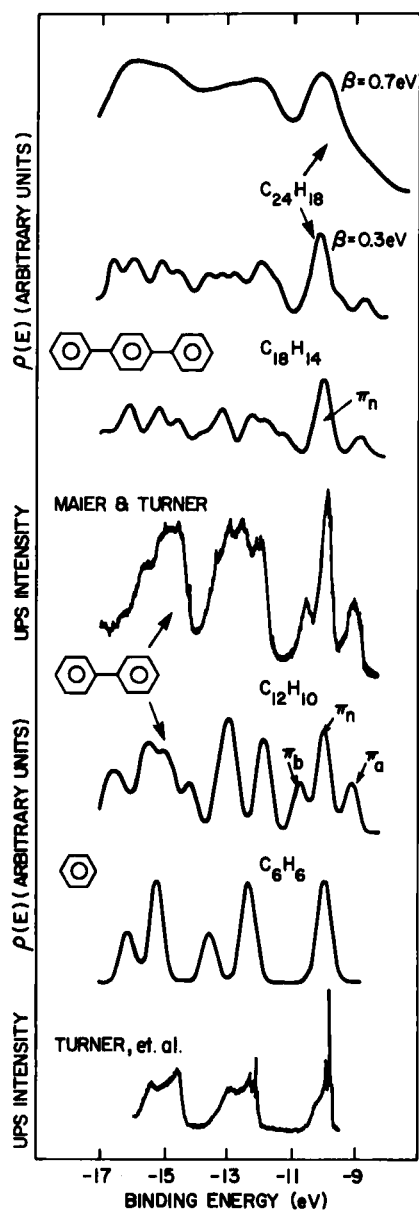
of 0.11 - 0.12 e for the other two carbon species in the backbone and to a uniform value of 0.09 e for the carbons in $(CH)_x$. The predicted increase in chemical instability of poly(1,6-heptadiyne)_x relative to polyacetylene is consistent with available data,²⁰ but the predicted changes in the DOVS and the red shift of the lowest energy $\pi \rightarrow \pi^*$ transition have not yet been either verified or disproved.

AROMATIC RING SYSTEMS WITH SATURATED LINKAGES

Another class of polymer matrices which has received considerable attention^{12,13,21} as suitable hosts for dopants is that based upon incorporating unsaturated pi-electron ring systems (e.g., phenyl moieties) into otherwise saturated backbones [e.g., poly(p-xylylene), bisphenol-A polycarbonate], attaching them together directly to form polymer chains [e.g., poly(p-phenylene), poly(2,5-thienylene)], or attaching them as pendant groups to a saturated-backbone [e.g., polystyrene, poly(N-vinyl carbazole), poly(2-vinyl pyridine)]. If the linkages are more effective than the fluctuations in the molecular ion energies on the individual rings, an extended-state polymer results.^{4,6,7,21} If not, the electronic states of the polymer are molecular cations and anions localized at individual sites along the polymer backbone.^{12,13,21} Therefore the suitability of such materials for doping to high conductivity depends on the effectiveness of the linkages, the degree of disorder in the solid-state polymer, and the influence of the dopant on both the structure and disorder of the initial polymer. Indeed these materials span the entire range from tolerable conductors when heavily doped [poly(p-phenylene)] to Fermi glasses exhibiting range-limited transport [undoped polystyrene, poly(2-vinyl pyridine)]. In this section we illustrate two main aspects of the dependence of the effectiveness of the linkages on molecular structure. First, we show how the pi-electron molecular ion states go from delocalized to localized in poly(p-phenylene) as opposed to poly(p-xylylene). Second, we illustrate the effect of heteroatoms in the aromatic ring by considering poly(2,5-thienylene). A detailed discussion of localization in pendant-group polymers like polystyrene has been given elsewhere,^{12,13,21} and hence is not reiterated here.

The presence of the phenyl moieties in the backbone of poly(p-phenylene), designated by $(C_6H_4)_x$, results in pi-electron molecular cation states which are fundamentally different from those obtained for polyacetylene chains. The doubly degenerate highest-energy $e_g(\pi)$ molecular orbital in benzene consists of a "non-bonding" orbital (indicated by π_u) which exhibits nodes at carbon atoms forming the links with the

FIGURE 5. Calculated CNDO/S3 DOVS for a series of poly-phenyls, $H(C_6H_4)_nH$ which become poly(p-phenylene) in the limit of large n . The molecules are taken as planar, and comparison is made with available gas-phase ultraviolet photoemission spectra for benzene²² and diphenyl.²³ The gas-phase spectra in the figure are shifted to higher binding energy by about 1 eV in order to retain the same energy scale in all the figures. Evaluation of the DOVS is described in the text and the caption for Fig. 4.



neighboring phenyl moieties, and a "bonding" orbital which exhibits maximum amplitude at these linking carbon species. In diphenyl, for which the calculated DOVS and observed gas-phase ultraviolet photoemission spectra are shown in Fig. 5, the non-bonding molecular ion states remain near the energy (-9.25 eV) of the corresponding molecular ion state in benzene whereas the bonding orbitals form antibonding (antisymmetric, π_a) and bonding (symmetric, π_b) molecular ion states as noted in the figure. This behavior persists as longer oligomers are built-up, leading to an intense narrow non-bonding π band in the center of a "bonding" π band for $(C_6H_4)_x$. As shown in the upper two panels of Fig. 5, the non-bonding π band is predicted to be a prominent feature of the DOVS of $(C_6H_4)_x$, although the bonding π band is so broad that its intensity gets smeared out in the solid state. No photoemission spectra are yet available to test the validity of these predictions for $(C_6H_4)_x$.

The coupling between the phenyl moieties in poly(p-phenylene) can be reduced by inserting saturated hydrocarbons in between them. Poly(p-xylylene) has an ethyl linkage between its phenyl moieties. It is a convenient material to study because of its ease of fabrication by vapor-phase pyrolysis of [2.2]Paracyclophane.²⁴ The valence electron photoemission spectrum of material prepared in this way is compared with model DOVS calculations and analogous spectra of vapor-phase²⁵ and solid-state²⁶ p-xylene in Fig. 6. It is evident from Fig. 6 that for $1 \text{ eV} \leq \beta \leq 1.2 \text{ eV}$ the DOVS of p-xylene and 1,2-di(p-tolyl)ethane are in good correspondence with the UPS data from condensed p-xylene and thin-film poly(p-xylylene). Moreover, for fixed values $\beta \sim 0.7 \text{ eV}$ the DOVS of p-xylene and oligomers of poly(p-xylylene) are indistinguishable. We infer, therefore, that the π -electron locations near $I_{\pi} = 7.5 \text{ eV}$ are localized on the individual phenyl moieties both in condensed p-xylene and in poly(p-xylylene) films, i.e., the ethyl linkages between the phenyl moieties in poly(p-xylylene) have reduced the coupling between them to the point that the bonding π band has a width comparable to the non-bonding π band, and both widths are small relative to the fluctuations in the relaxation energies of localized pi-electron phenyl radical cations.

We next turn to our last topic in this section, the effects of heteroatoms in the unsaturated rings. The contributions to the DOVS from the bonding π bands in ring architectures like the polyphenyls can be rendered more similar to the π bands in chain architectures like polyacetylene by utilizing asymmetric rings. A good example of this possibility is poly(2,5-thienylene) which is comprised of thiophene molecules in a

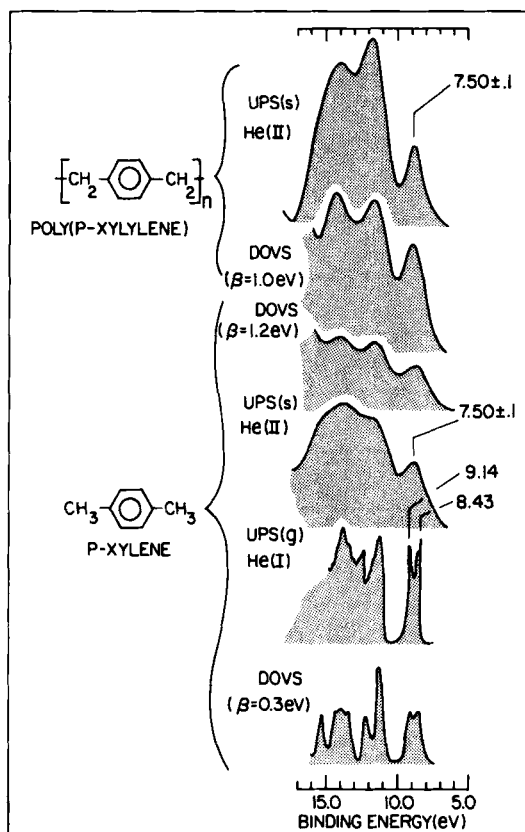
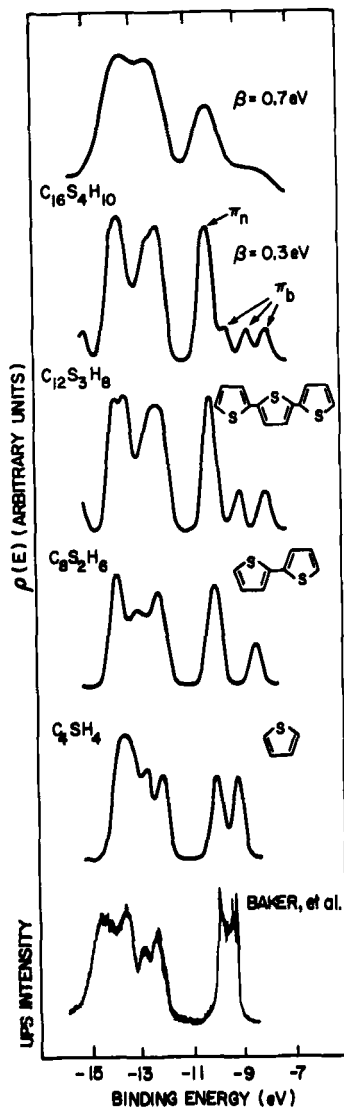


FIGURE 6. Comparison of measured ultraviolet photoemission spectra of gas-phase p-xylylene²⁵ (second panel), condensed phase p-xylylene²⁶ (third panel), and thin-film poly(p-xylylene)²⁶ (top panel) with densities of valence states (DOVS) calculated using the CNDO/S3 molecular orbital model.²⁶ The calculations corresponding to the gas-phase spectra utilize a gaussian of width $\beta = 0.03$ eV to represent each molecular-ion eigenvalue (lower panel). Those corresponding to the condensed phase spectra in the fourth and fifth panels embody $\beta = 1.2$ eV and 1.0 eV, respectively. The calculated DOVS labelled poly(p-xylylene) in the fifth panel of the figure was calculated for the p-xylylene²⁷ dimer 1,2-di(p-tolyl)ethane using an experimental geometry²⁷ corresponding to the β modification of poly(p-xylylene).²⁸ All of the spectra have been shifted to align them with the gas-phase results. The energies of the lowest π -electron ionization peaks for the condensed phase spectra are indicated in the figure.

FIGURE 7. Calculated CNDO/S3 DOVS for a series of polythienyls, $H(C_4H_2S)_nH$ ($n=1,2,3$ and 4), which become poly(2,5-thienylene) in the limit of large n . A symmetrized version of the structure of thiophene²⁹ and an antisymmetric planar orientation of the thienyl moieties³⁰ were utilized in the calculation. For thiophene, comparison with the ultraviolet photoemission spectrum of Baker *et al.*,³¹ is shown in the lower two panels. The photoemission spectrum is shifted to higher binding energies by 0.5 eV in order to retain the same energy scale in all of the figures. Evaluation of the DOVS is described in the text and in the caption to Fig. 4.



fashion analogous to the construction of poly(p-phenylene) from benzene rings. For thiophene the two highest-energy orbitals (corresponding to the $e_g(\pi)$ orbitals in benzene) are π orbitals with a nodal plane through the sulfur and the center of the back C-C bond, and with a nodal plane through the two carbon atoms adjacent to the sulfur, respectively. These orbitals correspond to the two isolated low-binding-energy ionizations between 9 eV and 10 eV evident in the lower two panels of Fig. 7. The highest-energy thiophene orbital

generates a "bonding" π band in the polythienyls nearly identical to the upper portion of the π band in trans-cisoid/transoid polyenes. The lower portion of the polyene bonding π band is greatly distorted in the polythienyls, however, because the totally symmetric π orbital in thiophene contains a substantial admixture of the sulfur p_z orbital. Thus, the main effect of heteroatoms in the unsaturated ring is to distort the bonding π bands relative to the phenyl ring systems. In the particular case of poly(2,5-thienylene), this distortion makes the upper part of the bonding π band similar to that in polyacetylene, thereby providing a ring molecular architecture whose electronic structure is analogous to that of a comparable chain architecture.

As in the case of the polyphenyls, the non-bonding molecular ion state in thiophene (the ionization peak near 10 eV binding energy in Fig. 7) remains nearly invariant as polythienyls are formed by joining multiple thiophene rings. In $(C_4SH_2)_x$, it becomes a non-bonding band (π^*) which is a prominent feature of the calculated DOVS as shown in the upper four panels of Fig. 7. In this particular case, the non-bonding π band lies at the high-binding-energy extremity of the low-binding-energy bonding π band. This behavior is similar to that observed at low binding energies in the phenylene oxides and sulfides, as may be discerned upon comparison of Fig. 7 with Fig. 8.

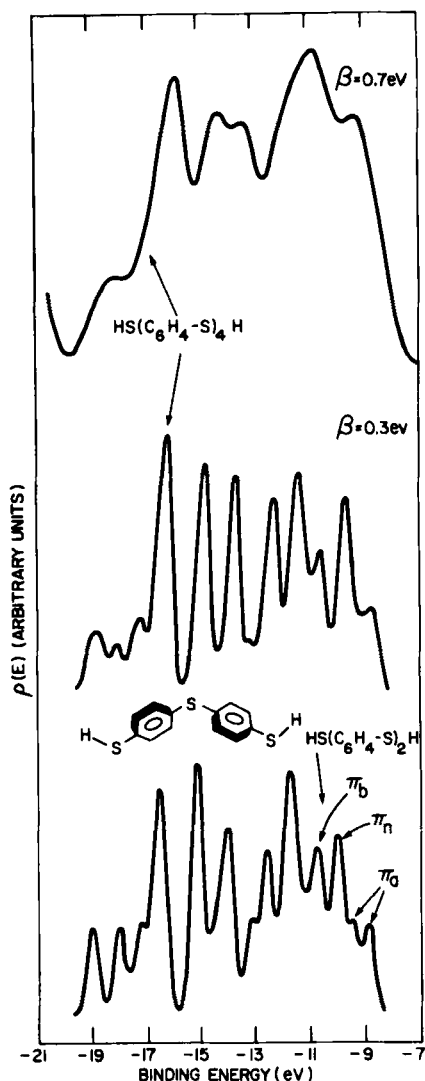
AROMATIC RING SYSTEMS WITH LONE-PAIR OR UNSATURATED LINKAGES

In the preceeding section we found that as the phenyl moieties in poly(p-phenylene) were separated by saturated linkages, the bonding π bands collapsed and ultimately the polymers became Fermi glasses with injected charges forming localized molecular ion states. Such need not be the case if the linkages are unsaturated or have lone pair electrons which can hybridize with the bonding π orbitals on the phenyl rings. Good examples of this phenomenon are the phenylene oxides and sulfides, as well as poly(p-phenylene vinylene). We consider these materials in this section.

The CNDO/S3 predictions for $(C_6H_4-O)_x$ and $(C_6H_4-S)_x$ are quite comparable to those for $(C_6H_4)_x$. The calculated DOVS for oligomers of poly(p-phenylene sulfide) are shown in Fig. 8. In these cases, however, the bonding π band is split into two parts, depending upon whether the phenyl π -electron linkages with the p orbitals on the chalcogens are bonding (π) or antibonding (π^*) in character. As in the case of $(C_6H_4)_x$, the most prominent π -electron contribution to the DOVS is

predicted to be the strong, sharp peak caused by the non-bonding π molecular ion states. Also as in the case of $(C_6H_4)_x$, the lower-binding-energy antibonding π -electron states are smeared out to the point of being hard to identify in the DOVS in the solid state. For $(C_6H_4)_x$, $(C_6H_4-O)_x$ and $(C_6H_4-S)_x$ all three, however, the CNDO/S3 model predicts that the lowest-binding-energy molecular ion states are π -electron states which extend throughout multiple monomolecu-

FIGURE 8. Calculated CNDO/S3 DOVS for the dimer and tetramer ($n=2$ and 4) derived from $HS(C_6H_4-S)_nH$ which corresponds to n poly(*p*-phenylene sulfide) in the limit of large n . A published structure of the polymer³² was used to construct the oligomers. Evaluation of the DOVS is described in the text and the caption for Fig. 4.



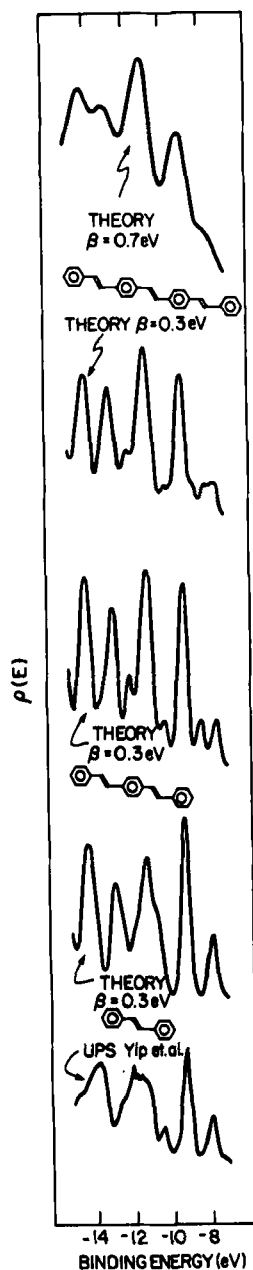
lar repeat units. Therefore the doping of these materials with acceptors in principle could produce electrical behavior comparable to that observed in polyacetylene. If the localized non-bonding π -electron states had exhibited the lowest binding energies, we would have anticipated difficulty in achieving high conductivities and mobilities via acceptor doping.

Finally, in Fig. 9 we show the analogous results for poly(p-phenylene vinylene). As in the case of diphenyl, the non-bonding π band is well resolved already for the dimer, stilbene. The pi-electrons on the ethyl linkages hybridize effectively with the bonding π electrons on the phenyl moieties for the planar geometry shown in Fig. 9. Obviously this hybridization depends sensitively on the phenyl-ethyl conformation, and would disappear if the two were orthogonal. Nevertheless, a wide π band can result even if phenyl moieties are widely separated, as is known to be the case for the diphenyl polyenes.³³

SYNOPSIS

The localized or extended character of the wave function of charges injected into a polymer is determined by the interplay between disorder-induced fluctuations in the site energies of localized molecular ions at the various sites along the polymer chains and the linkages between these sites both on the same chain and on different chains. Of the polymers considered herein the best possibilities for achieving extended states are predicted to occur in polyacetylene, poly(2,5-thienylene), poly(p-phenylene), and poly(p-phenylene vinylene) due to their high-energy pi-electron donor bands, although the latter three are more sensitive to conformational disorder than the former. The non-bonding pi-electron bands characteristic of unsaturated ring polymers, while prominent in the ultraviolet photoemission spectra, are not particularly useful in achieving either dopability or high mobility. For undoped polymers in the solid state, injected charges will reside in disorder-induced localized states at the edges of bands of allowed states, although the occurrence of massive charge transfer may enable the accessing of extended states nearer the center of the band to form "dirty" (i.e., low mobility) metals.⁴ If the linkages between the molecular ion sites on the backbone are too weak, however, all the states associated with injected charges are localized at individual sites along the polymer chain and a Fermi glass is formed. Examples of this limit are thought to be pi-electron states in poly(p-xylylene),¹³ polystyrene¹³ and poly(2-vinyl pyridine).²⁶ The presence of dopants adds additional disorder to the already disordered

FIGURE 9. Calculated CNDO/S3 DOVS for a series of oligomers of poly(p-phenylene-vinylene), $H[(C_6H_4)C_2H_2]_n C_6H_5$ ($n=1, 2$ and 3), which become poly(p-phenylene vinylene) in the limit of large n . For stilbene, comparison with the ultraviolet photoemission spectrum of Yip et al.,³³ is shown in the lower two panels. The photoemission spectrum is shifted to higher binding energies by 1.01 eV in order to retain the same energy scale in all of the figures. Evaluation of the DOVS is described in the text and in the caption to Fig. 4.



polymer chains, thereby rendering the criteria for extended ("band-like") states still more stringent. The morphology of the polymer is a critical ingredient in the doping process, with fibrillar morphologies like that of polyacetylene being unusually well suited to the achievement of high doping levels by virtue of the adsorption of the dopants at the surfaces of the fibrils, possibly resulting in conducting surface channels.^{3,4} Thus, we can say that open morphologies to facilitate high dopant concentration, low (high) site energies for acceptor (donor) polymer matrices, and strong (i.e., intimate) linkages between nearest-neighbor molecular ion sites all are necessary criteria for achieving high conductivity in molecularly doped polymers. Two of these criteria, those of the low (high)-site energies and intimate site linkages, imply chemical instability of the polymer upon doping, and the latter also suggests the lack of mechanical flexibility. Consequently, design of a stable, flexible, conducting polymer requires tailoring the linkages between local molecular ion sites [e.g., the S species in poly(p-phenylene sulfide)] to provide good electronic mixing between these sites but yet to remain both stable and flexible under dopant induced charge transfer. This felicitous combination of properties has not yet been demonstrated in the polymer-dopant systems studies thus far,¹⁻⁴ although an understanding of the molecular origin of the various properties enables systematic synthetic approaches to their simultaneous acquisition.

REFERENCES

1. C.B. Duke and H.W. Gibson, in Encyclopedia of Chemical Technology, (Wiley, New York, 1981).
2. R.H. Baughman, R.R. Chance, R.L. Elsenbaumer, D.M. Ivory, G.G. Miller, A.F. Preziosi and L.W. Shacklette, Org. Coat. Plast. Chem. 43, 762 (1980).
3. G.B. Street and T.C. Clarke, IBM J. Res. Develop. 25, 51 (1981).
4. C.B. Duke, in Extended Linear Chain Conductors. J.S. Miller, ed., (Plenum, New York, 1981), Vol. 2, pp. 59-125.
5. C.B. Duke, W.R. Salaneck, A. Paton, K.S. Liang, N.O. Lipari and R. Zallen, in Structure and Excitations of Amorphous Solids, G. Lucovsky and F. Galeener, eds., (AIP, New York, 1976), pp. 23-30.
6. C.B. Duke and A. Paton, Org. Coat. Plast. Chem. 43, 863 (1980); in Conducting Polymers, R.B. Seymour, ed. (Plenum, New York, 1981).
7. C.B. Duke, A. Paton, W.R. Salaneck, H.R. Thomas, E.W. Plummer, A.J. Heeger and A.G. MacDiarmid, Chem.

8. Phys. Lett. 59, 146 (1978).
8. J.J. Pireaux and R. Caudano, Phys. Rev. B 15, 2242 (1977).
9. C.B. Duke, Int. Jour. Quant. Chem.: Quant. Chem. Symposm. 13, 267 (1979).
10. P.M. Grant and I.P. Batra, Synthetic Metals 1, 193 (1979/80).
11. J.L. Bredas, R.R. Chance, R.H. Baughman and R. Silbey, J. Am. Chem. Soc. (to be published).
12. C.B. Duke, A. Paton, and T.J. Fabish, Chem. Phys. Lett. 49, 133 (1977).
13. C.B. Duke, W.R. Salaneck, T.J. Fabish, J.J. Ritsko, H.R. Thomas and A. Paton, Phys. Rev. B 18, 5717 (1978).
14. W.R. Salaneck, C.B. Duke, W. Eberhardt, E.W. Plummer and H.J. Freund, Phys. Rev. Lett. 45, 280 (1980).
15. L.E. Sutton, ed., Tables of Interatomic Distances and Configuration in Molecules and Ions (Chemical Society, London, 1958).
16. J.M. Andre, Polym. Preprints 21, 127 (1980).
17. T. Ito, H. Shirakawa and S. Ikeda, J. Polym. Sci. Polym. Chem. Ed. 13, 1943 (1975).
18. D. Vanderbilt and E. Mele, Phys. Rev. B 22, 3939 (1980).
19. W.R. Salaneck, H.W. Gibson, C.B. Duke, F. Greuter and W. Eberhardt, Bull. Am. Phys. Soc. 26, 346 (1981).
20. H.W. Gibson, F.C. Bailey, J.M. Pochan, A.J. Epstein and H. Rommelmann, Organic Coatings and Plastics Chemistry Preprints 42, 603 (1980).
21. C.B. Duke, Surface Sci. 70, 674 (1978); Mol. Cryst. Liq. Cryst. 50, 63 (1979).
22. D.W. Turner, C. Baker, A.D. Baker and C.R. Brundle, Molecular Photoelectron Spectroscopy (Wiley Interscience, London, 1970), p.271.
23. J.P. Maier and D.W. Turner, Farad. Disc. Chem. Soc. 54, 149 (1972).
24. W.G. Gorham, in Encyclopedia of Polymer Science and Technology, H.F. Mark, N.G. Gaylord and N. Bikales, eds., (Interscience, New York, 1971), Vol. 15, pp. 98-113.
25. T. Koenig, M. Tuttle and R.A. Wielessek, Tetrahedron Lett. 29, 2537 (1974).
26. C.B. Duke, R.W. Bigelow, A. Dilks, A. Paton, W.R. Salaneck and H.R. Thomas, Chem. Phys. Lett. (in press).
27. C.J. Brown, Acta. Cryst. 7, 97 (1954).
28. W.D. Niegisch, in Encyclopedia of Polymer Science and Technology, H.F. Mark, N.G. Gaylord and N. Bikales, eds., (Interscience, New York, 1971), Vol. 15, pp. 113-124.
29. B. Bak, D. Christensen, L. Hansen-Nygaard and J. Rastrup-Andersen, Jour. Mol. Spectros. 7, 58 (1961).

30. G.J. Visser, G.J. Heeres, J. Wolters and A. Vos, Acta. Cryst. B 24, 467 (1968).
31. A.D. Baker, D. Betteridge, N.R. Kemp and R.E. Kirby, Anal. Chem. 42, 1064 (1970).
32. B.J. Tabor, E.P. Magre and J. Boon, Eur. Polym. Jour. 7, 1127 (1971).
33. K.L. Yip, N.O. Lipari, C.B. Duke, B.S. Hudson and J. Diamond, J. Chem. Phys. 64, 4020 (1976).
34. W.R. Salaneck, H.R. Thomas, C.B. Duke, A. Paton, E.W. Plummer, A.J. Heeger and A.G. MacDiarmid, J. Chem. Phys. 71, 2044 (1979).